

# SENSITIVITY TO CONTACT GEOMETRY OF THE TRANSVERSE CURRENT DISTRIBUTION INTO A BSCCO TAPE: A COMPUTATIONAL STUDY

## SENSIBILIDAD A LA GEOMETRÍA DE LOS CONTACTOS DE LA DISTRIBUCIÓN DE CORRIENTE TRANSVERSAL EN CINTAS DE BSCCO: UN ESTUDIO COMPUTACIONAL

A. S. GARCÍA-GORDILLO<sup>at</sup>, A. REYES<sup>a</sup> AND E. ALTSHULER<sup>a</sup>

Superconductivity Laboratory, Physics Faculty-IMRE, University of Havana, 10400 Havana, Cuba. andy.garcia@fisica.uh.cu<sup>†</sup>

Recibido /04/2019; Aceptado //2019

PACS: Superconducting wires, fibers and tapes (cables, fibras y cintas superconductoras), 84.71.Mn; Superconductor transport properties, transport processes in superconductors (propiedades de transporte superconductor, procesos de transporte en superconductores), 74.25.F-; Numerical simulations studies (estudios de simulación numérica), 75.40.Mg

The four-probe technique is a standard way for measuring transport properties in samples with low output voltage. The use of this technique to study inhomogeneities of superconducting properties of ceramic superconductors [1–6], coated superconductors [7,8], films [9,10] and tapes [11,12] has been well established. A less common practice in the study of these materials is to change the positions of the voltage probes in order to explore local properties. A study of the local transport properties in the transverse direction of  $Bi_2Sr_2Ca_2Cu_3O_{10+x}$  tapes [13] and some studies related to the anisotropy in the dissipation associated to transport currents in the longitudinal and transverse directions on multi-filamentary  $Bi_2Sr_2Ca_2Cu_3O_{10+x}$  tapes [14, 15] were accomplished by changing the position of the voltage probes in the four-probes set-up. However, very small attention has been put in studying the effects of the positions of the *current* leads on the transport measurements and sample performance. Particularly, it is interesting to know how the current injection geometry may influence the formation of hot spots [16] and the shape of the I - V curves.

Understanding the onset of hot spots under different experimental conditions is very relevant, since local overheating has always been an important issue in the behavior of superconducting magnets and power transmission lines. The transverse direction in the presence of transverse cracks [17, 18] constitutes “an escape way” for the current. To study the transport properties of the tape when current meets one of these cracks it is required to inject current in the transverse direction.

In the present paper we study by means of numerical simulations the sensitivity of the current distribution inside a  $Bi_2Sr_2Ca_2Cu_3O_{10+x}/Ag$  multi-filamentary superconducting tape when an external current flows transverse to the superconducting filaments. It is possible by using a transverse bridge, i.e., a slice of a superconducting tape cut perpendicular to the filaments [13–15, 19].

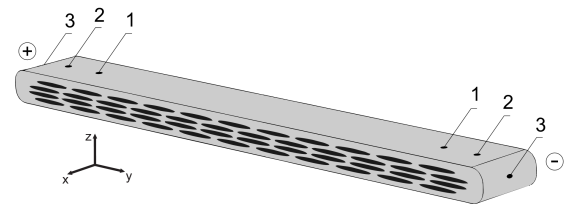


Figure 1. Sketch of a transverse bridge on a multi-filamentary tape. The pairs of current probes labelled as “1”, “2” and “3” correspond to Configurations 1, 2 and 3, respectively, and the current flows in the direction from “+” to “-”. The dimensions along x, y and z of the bridge in a real sample are of 0.5 mm, 4.32 mm and 0.23 mm, respectively.

The transverse bridge used in the simulations replicated quite precisely the cross-section of the BSCCO tape used by us in previous experiments [19]. It was 4.32 mm wide and 0.23 mm thick, and contained 46 elliptical cross-sectioned filaments. All the filaments were identical, each one 0.3 mm wide and 25 microns thick, giving a filling factor of  $S_{BSCCO}/S_0 = 0.27$ , where  $S_{BSCCO}$  is the cross-section area of the superconductor and  $S_0$  is the whole cross-section of the tape. The width of the bridge (i.e., its size parallel to the main direction of the tape) was 0.5 mm.

COMSOL Multiphysics was used to run the simulations. It uses the FEM (Finite Elements Method) to solve the stationary electrical problem we are aiming at. Three different current probes configurations were set in order to explore the current distribution inside the bridge.

Figure 1 shows a sketch of the transverse bridge where the current probes configurations are depicted. In ‘Configuration 1’ the probes are located on top of the tape, close to the edges of the transverse bridge, directly over the gap of the two closest filaments. ‘Configuration 2’ is quite similar to the first one: the probes are also on top of the tape. However, they are closer to the edges of the transverse bridge in such a way that each probe has only one filament directly underneath it. In ‘Configuration 3’, the probes are located at the center of the sides of the transverse bridge.

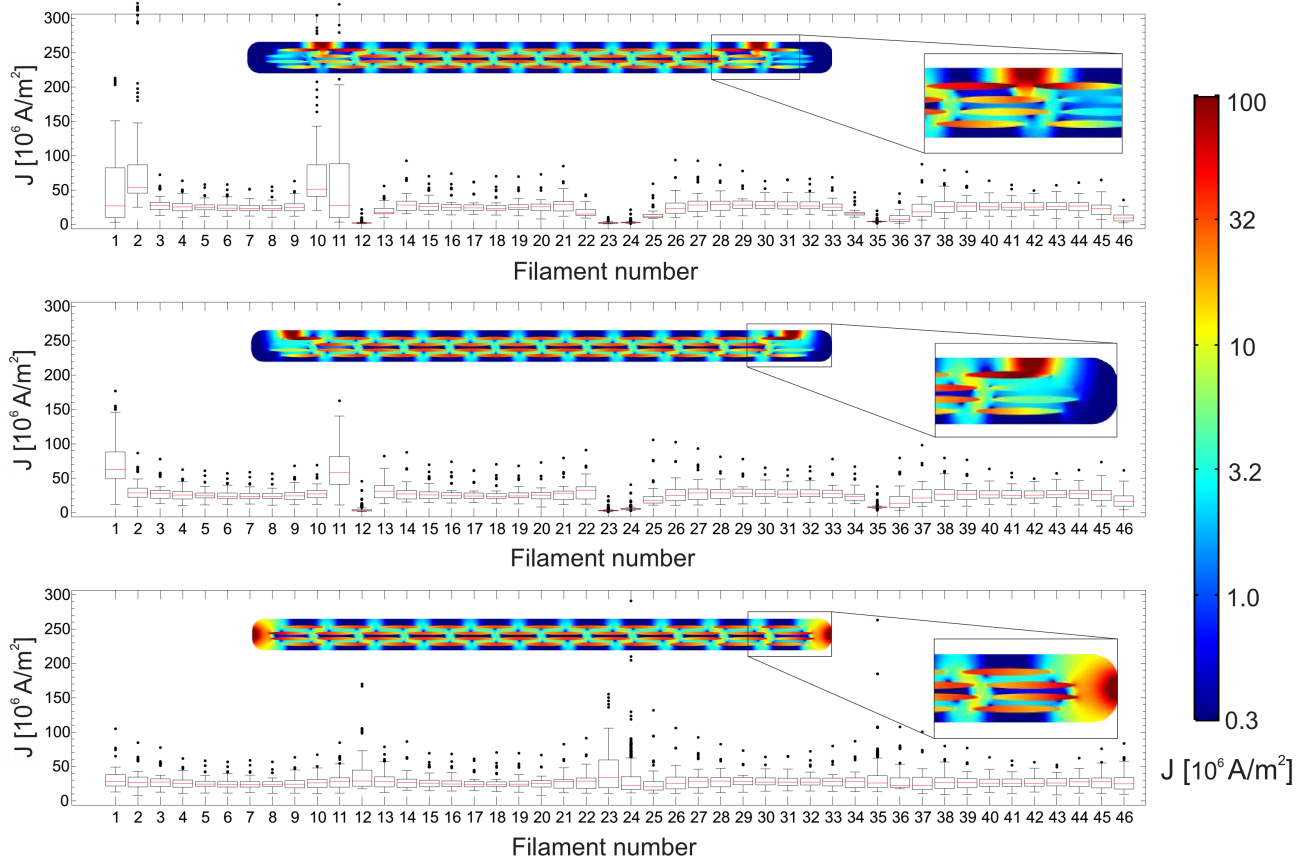


Figure 2. Detailed current density distributions for configurations 1, 2 and 3, from top to bottom. Each graph consists in a box diagram showing the current densities circulating through each filament (boxes from 1 to 11 correspond to the first 11 filaments of the top row, counting from left to right; boxes from 12 to 23 correspond to the second row of 12 filaments, counting from left to right, and so on). The central insets show a transversal cut of the bridge, where the current density module follows the color code indicated by the bar at the far right. The right insets are zooms of the current density distribution near the right contacts.

The superconducting filaments were modeled as normal conductors with high conductivity values, and the material surrounding was modeled as silver with a  $\sigma = 3.44 \times 10^8$  S/m (at liquid nitrogen temperature [20]). The conductivity values of the filaments exceeded in six orders the ones of the silver. The bias current was set to 1 A in the three configurations. That value is supposed to be lower than the value of the critical current, so that the filaments remain in the superconducting state. Silver was chosen in order to reproduce the original tape, but different values of the superconductor and metal conductivities could have been used instead. However, the results are robust if the two conductivities differ by five orders of magnitude or more.

The current density through the filaments and the silver matrix was calculated for the three configurations. Aimed at decreasing the calculation time, all data was calculated exclusively within the plane including the current probes. Due to the geometry partition into small domains made by the program to solve the continuity equation in a discrete way using the FEM, a mean of 650 values of current density can be extracted from each filament in that slice. Filaments are numbered in the computational model for a better understanding of the spatial current density distribution. If we imagine the cross-section of the tape, as seen in the transverse bridge of figure 1, filaments are numbered from left to right and from top to bottom. The top row of filaments

goes from 1 to 11, second one goes from 12 to 23, third from 24 to 35, and the bottom row goes from filament 36 to 46.

Figure 2 shows, for the three configurations, box whisker charts with the distributions of the current density values inside each filament. ‘Configuration 1’, ‘2’ and ‘3’ are shown in the top, middle and bottom panels respectively. Each chart has an inset containing a color graph with a map of the current density distribution inside the whole transverse bridge center slice. A global legend at the right of the graphs illustrates the color scale of the insets current density distribution. The convention used for whiskers and outliers was taken according to Tukey’s method [21], in which if  $Q_1$  and  $Q_3$  are the lower and upper quartiles of the data set respectively, then one could define an outlier to be any observation outside the range:  $[Q_1 - k(Q_3 - Q_1), Q_3 + k(Q_3 - Q_1)]$  where  $k = 1.5$  defines the points that will be considered outliers and  $k = 3$  those classified as “far out”.

In ‘Configuration 1’ current distributes all over the transverse bridge with a visible increase of the current density values inside four filaments at the top row, as seen from the medians and the tails of the current density distributions shown in the box whisker chart. The filaments with high current density values are the ones located immediately underneath the current probes, indicating that current flows almost entirely through them, and then redistributes among the rest of the filaments. We can confirm this by analysing the centered

slice color graph in the inset. In 'Configuration 2' the current density distribution exhibits a similar behavior resulting in a pair of filaments with high current density values. The medians of the distributions inside these filaments are larger than in 'Configuration 1', which seems obvious if we take into account that the current is sustained almost entirely by two filaments instead of four, as can be seen from the inset. These values are not substantially different from each other since the current density median of filament 2 in 'Configuration 1' is approximately  $53.6 \times 10^6 A/m^2$  and the current density median of filament 1 in 'Configuration 2' is approximately  $63 \times 10^6 A/m^2$ ; but the slightest difference may start the transition. 'Configuration 3', on the other hand, does not show a high concentration of current in very few filaments: they have current density distributions with almost the same median and, in general, they show short tails. The difference with previous configurations can be explained by the fact that the contacts are located at the center of the sides of the transverse bridge -relatively far from any particular group of filaments- which allows the current to flow a certain distance inside the silver and reach, in a more homogenized way, a larger number of filaments.

Thus, filaments below current probes in configurations 1 and 2 constitute regions of local overheating -hot spots- which may compromise the conduction in the transverse direction of the tape. If we look closely at the color graphs in the insets of Figure 2 we can see that inside these filaments there are regions with very high current density values corresponding to these hot spots but also there are regions of silver and filaments with substantially lower current density values. These "cold" regions that can be viewed as "reservoirs" of conductive paths, have an effect in the velocity of the transition to the normal state. So, in principle, they can prevent a "fatal rupture" of the tapes when transversal cracks are present.

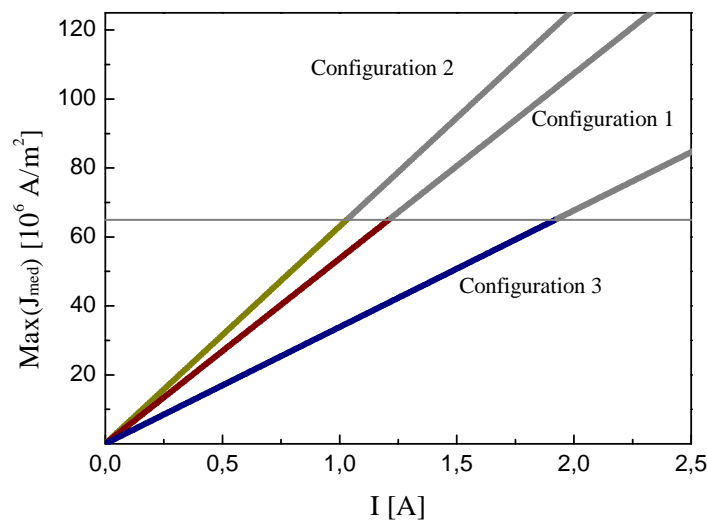


Figure 3. Dependence of the maximum of the current density distributions medians with the applied current. The red curve corresponds to 'Configuration 1', the yellow one corresponds to 'Configuration 2' and the blue one belongs to 'Configuration 3'.  $J_c$  is marked with a gray horizontal line. The inset shows the behavior of the maximum of the current density distributions upper fences.

A parametric study related to the medians of the current density distributions inside the filaments endorse the fact that the characterization curves are strongly conditioned by the position of the current probes. Applied current was varied from 0 to 2.5 A in order to find out which of these configurations allow us to reach the critical current density 'earlier', under realistic experimental parameters [13–15,19].

Figure 3 shows the behavior of the maximum of the current density distributions medians among all filaments ( $\text{Max}(J_{\text{med}})$ ) with the applied current (I). The curves for the different configurations are labeled in the graph, showing that the red curve corresponds to 'Configuration 1', the yellow one corresponds to 'Configuration 2' and the blue one belongs to 'Configuration 3'. The maxima of the current density distributions medians were always found in the same filament according to the corresponding configuration. In 'Configuration 1' the maximum was found in filament number 2, 'Configuration 2' presented its maximum in filament 1 and in 'Configuration 3' the maximum was on filament 23. These are the filaments which have the highest median values in each configuration. It is important to mention that despite of the symmetry in the position of the current probes, filaments below the right and the left probes do not hold exactly the same current density because we realistically reproduced the filament distribution of a real tape, which includes a slight asymmetry in the filament distribution. Hence, in configurations 1 and 2 the important filaments are below the left current probe, and, in 'Configuration 3', the filament with the highest median is placed at the left of the right probe.

If we assume the critical current density ( $J_c$ ) of the filaments equals to  $239.8 \times 10^6 A/m^2$  (calculated from the  $S_{BSCCO}/S_0$  ratio and the engineering critical current of the BSCCO multi-filamentary superconducting tape at liquid nitrogen temperature [15] -marked in the graph as a gray horizontal line-) we can see from Figure 3 that  $J_c$  is reached first in 'Configuration 2'. This will switch at least one filament out of the superconducting state, redistributing the current density to neighboring filaments. As the applied current increases this redistribution involves more filaments, giving rise to a gradual transition of the full bridge to the normal state. This is in accordance with the box whisker charts of Figure 2 where the highest value of the medians corresponds to 'Configuration 2', followed by 'Configuration 1' and then 'Configuration 3', which needs a much larger current value to reach the critical current density. The difference can be unexpectedly large: Fig. 3 shows that the horizontal line intercepts 'Configuration 3' at approximately twice the current at which it intercepts 'Configuration 2'.

Although taking the medians of the distributions as reference parameters to compare the different configurations seems to be a reasonable decision because of the complexity of the transition to the normal state, the maximum deviation above medians might constitute a more suitable and interesting magnitude to evaluate this difference as well. The inset in Fig. 3 shows the dependence of the maximum of the current density distributions upper fences with the applied current, defining the upper fences as the values of current density at

the end of the upper whisker (maximum deviation above medians not including the outliers). The maxima of the upper fences [  $\text{Max}(J_{max})$  ] were always found in the same filament according to the corresponding configuration as in the medians study. However, relevant filaments were not the same. In configurations 2 and 3 the maximum was found in filaments number 1 and 23 respectively, but in 'Configuration 1', instead of in filament number 2, the maximum was found in filament number 11 (clearly visible from the box diagrams of Figure 2). The values of the maxima of the upper fences in 'Configuration 1' are larger than those of 'Configuration 2' changing the order in which the transitions out of the superconducting state occur in the different configurations. Additionally, the values of the intersections with the  $J_c$  horizontal line are way smaller if the upper fences are taken into account. It is quite difficult to tell which of these statistical magnitudes best describes the transition: while the study of the upper fences seems to give an onset of the transition, the medians offers a more "averaged out" data.

In summary, the sensitivity of the transverse current to different configurations of current probes in  $\text{Bi}_2\text{Sr}_2\text{Ca}_2\text{Cu}_3\text{O}_{10+x}/\text{Ag}$  multi-filamentary superconducting tapes was studied. Simulations strongly suggest that a configuration where the current probes are far from a particular group of filaments does not create hot spots; a desirable scenario for applications. In addition, the different values of applied current needed to reach the critical current density in the different configurations, as well as the different current distributions inside the transverse bridge of the tape suggest that the transverse transport characterization of a multi-filamentary tape is unexpectedly dependent on the detailed positioning of the current probes.

#### ACKNOWLEDGEMENTS

The authors thank A. Serrano-Muñoz and G. Viera-López for their suggestions about the color code in Figure 2.

#### REFERENCES

[1] J. R. Clem, *Physica C* **153-155 (part1)**, 50 (1988).  
 [2] E. Altshuler, R. Cobas, A. J. Batista-Leyva, C. Noda, L. E. Flores, C. Martínez and M. T. D. Orlando, *Phys. Rev. B* **60**, 3673 (1999).

[3] A. J. Batista-Leyva, R. Cobas, E. Estévez-Rams, M. T. D. Orlando, C. Noda and E. Altshuler, *Physica C* **331**, 57 (2000).  
 [4] A. J. Batista-Leyva, R. Cobas, M. T. D. Orlando and E. Altshuler, *Supercond. Sci. Technol.* **16**, 857 (2003).  
 [5] S. Recuero, N. Andrés, J. Lobera, M. P. Arroyo, L. A. Angurel, and F. Lera, *Meas. Sci. Technol.* **16**, 1030 (2005).  
 [6] W. Treimer, O. Ebrahimi and N. Karakas, *Appl. Phys. Lett.* **101**, 162603 (2012).  
 [7] S. Trommler, R. Hühne, E. Reich, K. Ida, S. Haidndl, V. Matias, L. Schultz and B. Holzapfel, *Appl. Phys. Lett.* **100**, 1226602 (2012).  
 [8] D. Colangelo and B. Dutoit, *Supercond. Sci. Technol.* **25**, 1 (2012).  
 [9] J. Hua, Z. L. Xiao, D. Rosenmann, I. Beloborodov, U. Welp, W. K. Kwok and G. W. Crabtree, *Appl. Phys. Lett.* **90**, 072507 (2007).  
 [10] T. Horide and K. Matsumoto, *Appl. Phys. Lett.* **101**, 112604 (2012).  
 [11] K. Ogawa and K. Osamura, *Phys. Rev. B* **67**, 184509 (2003).  
 [12] M. Zhang, J. Kvitkovic, J. H. Kim, C. H. Kim, S. V. Pamidi and T. A. Coombs, *Appl. Phys. Lett.* **101**, 102602 (2012).  
 [13] A. Borroto, L. Del Río, E. Altshuler, M. Arronte, P. Mikheenko, A. Qviller and T. H. Johansen, *Supercond. Sci. Technol.* **26**, 115004 (2013).  
 [14] A. Borroto, L. Del Río, M. Arronte, T. H. Johansen and E. Altshuler, *Appl. Phys. Lett.* **105**, 202604 (2014).  
 [15] A. Borroto, A. S. García-Gordillo, L. Del Río, M. Arronte, and E. Altshuler, *Supercond. Sci. Technol.* **28**, 075008 (2015).  
 [16] L. Del Río, E. Altshuler, S. Niratisairak, Ø. Haugen, T. H. Johansen, B. A. Davidson, G. Testa and E. Sarnelli, *Supercond. Sci. Technol.* **23**, 085005 (2010).  
 [17] X. Y. Cai, A. Polyanskii, Q. Li, G. N. Riley Jr and D. C. Larbalestier, *Nature* **392**, 906 (1998).  
 [18] H. Akiyama, Y. Tsuchiya, S. Pyon and T. Tamegai, *Physica C* **504**, 65 (2014).  
 [19] A. S. García-Gordillo, A. Borroto and E. Altshuler, *Rev. Cubana Fis.* **31**, 96 (2014).  
 [20] D. R. Smith and F. R. Fickett, *J. Res. Natl. Inst. Stand. Technol.* **100**, 119 (1995).  
 [21] J. W. Tukey, *Exploratory Data Analysis*, 1st Ed. (Addison-Wesley, 1977)

This work is licensed under the Creative Commons Attribution-NonCommercial 4.0 International (CC BY-NC 4.0, <http://creativecommons.org/licenses/by-nc/4.0>) license.

